Prospects for Nonlinear Energy Harvesting Systems Designed Near the Elastic Stability Limit When Driven by Colored Noise

R. L. Harne
e-mail: rharne@umich.edu

K. W. Wang

Department of Mechanical Engineering,
University of Michigan,
Ann Arbor, MI 48109-2125

Ambient vibration sources in many prime energy harvesting applications are characterized as having stochastic response with spectra concentrated at low frequencies and steadily reduced power density as frequency increases (colored noise). To overcome challenges in designing linear resonant systems for such inputs, nonlinear restoring potential shaping has become a popular means of extending a harvester's bandwidth downward towards the highest concentration of excitation energy available. Due to recent works which have individually probed by analysis, simulation, or experiment the opportunity for harvester restoring potential shaping near the elastic stability limit (buckling transition) to improve power generation in stochastic environments—in most cases focusing on postbuckled designs and in some cases arriving at conflicting conclusions—we seek to provide a consolidated and insightful investigation for energy harvester performance employing designs in this critical regime. Practical aspects drive the study and encourage evaluation of the role of asymmetries in restoring potential forms. New analytical, numerical, and experimental investigations are conducted and compared to rigorously assess the opportunities and reach well-informed conclusions. Weakly bistable systems are shown to potentially provide minor performance benefits but necessitate a priori knowledge of the excitation environment and careful avoidance of asymmetries. It is found that a system designed as close to the elastic stability limit as possible, without passing the buckling transition, may be the wiser solution to energy harvesting in colored noise environments. [DOI: 10.1115/1.4026212]

Keywords: nonlinear vibration energy harvesting, bistable, elastic instability, asymmetry

1 Introduction

The successful implementation of vibration energy harvesting systems relies on the matching of the device dynamics to the vibration spectra and form which excite the oscillators. Consequently, device development is best accomplished following realistic assessment of the input excitation source. While energy harvesting applications are too numerous to count, the critical applications are those for which it is genuinely infeasible to access the location by line transmission and when other power sources are ill-suited. For example, vibration energy harvesting in an urban environment may pose less cost-benefit attraction than achieving successful electrical power generation on a wireless weather station buoy far at sea or a health-monitoring sensor on a truss bridge span over a gorge. The ambient vibration sources to harness in these remote environments are often characterized by stochastic oscillations with peak amplitudes in the range of a few Hz or less [1–4]. Above the frequencies associated with peak acceleration amplitudes, the power spectra roll off at a rate of 20–40 dB/decade, which is characteristic of exponentially-correlated (colored) or quasi-monochromatic noise sources [5]. These are the key vibrational sources of interest which drive this study.

From an engineering design perspective, it is challenging to develop energy harvesters sensitive to such spectra. Fortunately, numerous recent investigations have uncovered promising opportunities utilizing nonlinear restoring force (or potential) shaping to heighten the sensitivity of harvesters to broader and lower excitation spectra [6,7]. Many studies have considered bistable harvesters which are postbuckled systems capable of undergoing energetic cross- or interwell responses [7]. In most cases, the conversion of nonlinear monostable harvester designs to bistable forms is achieved by gradually changing a design parameter proportional to a buckling force (e.g., an axial load upon a cantilevered harvester beam) until the critical load has been exceeded: passing the limit of elastic stability. Magnetic repulsion, magnetic attraction, and mechanical loading have been popular techniques to realize these effects [7–10]. The buckling process reduces the linear natural frequency of the system to a theoretical null at the critical transition [10]; at this point, the system is termed *essentially nonlinear* because linear restoring forces are eliminated. Quinn and colleagues [11,12] have investigated essentially nonlinear energy harvesters for harmonic and impulsive loading, but, given the sparse attention to harvester assessment within this specific design space, decisive conclusions on their performance in stochastic environments have yet to be made.

Some additional studies encourage further exploration regarding stochastically-excited nonlinear harvesters with restoring potentials designed near the elastic stability limit. Tang et al. [13] experimentally observed that when excited by *white noise*, a harvester beam having magnetic repulsion to buckle the system achieved "optimal performance… near the monostable-to-bistable transition region." Zhao and Erturk [14] demonstrated that the only instance in which a bistable harvester outperformed its linear counterpart in *white noise* environments was when the bistable system was excited to a degree to just allow the harvester mass to cross the double-well potential barrier and undergo random interwell vibration. This indicates that bistability is only beneficial if the well-escaping phenomena is consistently triggered which, in one method, may be achieved by designing a marginally or

Contributed by the Design Engineering Division of ASME for publication in the Journal of Vibration and Acoustics. Manuscript received May 27, 2013; final manuscript received November 26, 2013; published online December 24, 2013. Assoc. Editor: Brian P. Mann.

weakly bistable system in tandem with thoughtful assessment of the ambient excitation level. These prior empirical findings [13,14] deviate from theoretical studies by Daqaq [15–17] which indicate that nonlinear restoring potential shaping cannot improve power generation over linear harvesters in *white noise* environments for devices having large ratio of mechanical to electrical time constants, τ_m/τ_e, which represents all harvesters designed near the stability limit because $\tau_m/\tau_e \to \infty$ at the limit. Theory moreover suggests that bistable potential well shaping may enable a bistable harvester to outperform a linear counterpart in *colored noise* environments [16] and a recent numerical and experimental study has given initial evidence of such [18]. Finally, using measured stochastic excitations evincing *colored noise* characteristics as modeling inputs, Green et al. [19] recently concluded that designers must contend with the fact that ambient vibrations are concentrated at frequencies so low that any energy harvester configuration is challenged to be wholly effective for realistic excitations. From the above reviews, it is clear that there remains an important need to systematically and comprehensively evaluate the full opportunities of restoring potential shaping near the elastic stability limit, not specifically focused on bistability, under *colored noise* excitations (which are more representative of key ambient vibration sources than white noise) in order to form definitive conclusions on best energy harvesting system design practices.

Another practical factor plays a leading role in the present investigations. Realistic devices may most likely have asymmetries (consequently, *biases*) in their restoring potentials due to imperfections. Few authors report these features but a number have described asymmetric biases for bistable harvesters [8,20,21]. The imperfections may be caused by subtle details such as the straightness of the harvester beam, eccentricity of the buckling force, and even gravity. In spite of reports of asymmetries principally for bistable devices, these concerns are relevant both before and after the buckling transition. Consequently, in this work we find it critical to take into account the role of asymmetries on energy harvester performance near the elastic stability limit.

The previous findings and practical considerations collectively impel this work. We seek to determine the benefits of energy harvesting systems having restoring potentials designed near the elastic stability limit. As opposed to studies based on harmonic or white noise excitations [7–10,13,14,20–22], we are interested in the probability density functions (pdfs) and long-time mean-square responses of the systems due to colored noise excitations, representative of prominent ambient vibration sources existing in field settings for which vibration energy harvesting applications are well-suited. Since past analytical, numerical, and experimental works have individually reported varied, and sometimes conflicting, results regarding nonlinear energy harvesting performance in *white noise* environments, this paper provides and compares each evaluation form to synthesize comprehensive answers to the questions at hand crucial to successful power generation from realistic *colored noise* excitations.

Section 2 poses the problem formulation of the stochastic response of a nonlinear energy harvester having restoring potential of generic quartic shape and describes modeling assumptions. Stationary response pdfs are determined via established methods and experimental system details are provided. Then analytical, simulated, and experimental results for the response of nonlinear energy harvesters designed near the elastic stability limit are compared, followed by discussions on key findings.

2 Nonlinear Harvester Modeling

The nonlinear energy harvester architecture is depicted in Fig. 1, where a base-excited oscillator having nonlinear restoring force $f(k_0, k_1, k_3)$ includes piezoelectric and electromagnetic induction electromechanical conversion mechanisms configured to convert the relative kinetic energy between the harvester mass motion and moving base into electrical signal to be captured by external circuitry, here modeled as resistive loads. In this manner,

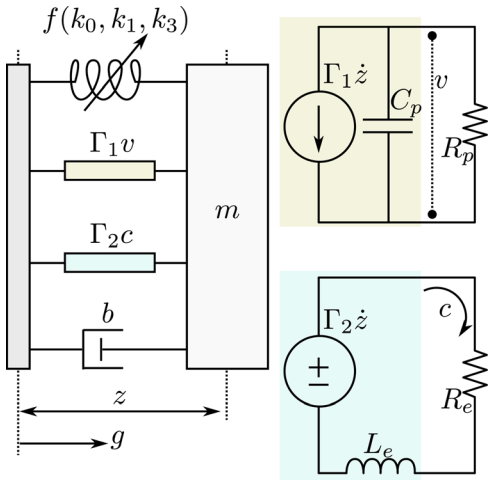

Fig. 1 Nonlinear energy harvester with piezoelectric and electromagnetic induction mechanisms and corresponding circuitry

findings of this work are applicable to the larger class of energy harvesting systems employing one or both of the above transduction techniques.

Equation (1) defines the response of the nonlinear harvester motion and circuit outputs.

$$m\ddot{z} + b\dot{z} + \bar{V}'(z) = -m\ddot{g} - \Gamma_1 v - \Gamma_2 c \tag{1a}$$

$$\bar{V}(z) = \int f(z)\mathrm{d}z = k_0 z - \frac{1}{2}k_1 z^2 + \frac{1}{4}k_3 z^4 \tag{1b}$$

$$C_p \dot{v} + \tfrac{1}{R_p} v = \Gamma_1 \dot{z} \tag{1c}$$

$$L_e \dot{c} + R_e c = \Gamma_2 \dot{z} \tag{1d}$$

Derivatives are expressed by $(\dot{}) = \mathrm{d}/\mathrm{d}t$ and $()' = \mathrm{d}/\mathrm{d}z$. The restoring potential $\bar{V}(z)$ neglects a cubic term in this investigation because prior studies indicate that probabilistic outcomes for systems having quartic potentials are substantially less influenced by asymmetries tending from cubic potential terms (or quadratic forces) as compared to linear terms (or static, bias forces) [23,24]. Biases, included here by coefficient k_0, are commonly encountered in practical energy harvesting system development, including biases imposed by gravitational loading or due to manufacturing imperfections.

An important modeling assumption is now applied in light of the focus of the present study. In targeting ambient vibration sources with greatest energy density in the sub-Hz range, we are interested in harvesters practically designed with natural frequencies as low as feasibly possible. As compared to available piezoelectric materials and electromagnetic induction harvester realizations, this implies that the mechanical time constants will often be significantly greater than the electrical time constants. In this context, the primary influence of either transduction is a dissipation of energy in the external circuit [16,25]. With this assumption in mind, Eq. (1) is reduced and rearranged.

$$\ddot{z} + \mu\dot{z} + V'(z) = \zeta(t) \tag{2a}$$

$$V(z) = \alpha z - \frac{1}{2}\kappa z^2 + \frac{1}{4}\beta z^4 \tag{2b}$$

$$\alpha = k_0/m, \quad \kappa = k_1/m, \quad \beta = k_3/m, \quad \mu = \frac{1}{m}(b + \phi) \tag{2c}$$

$$\phi = R_p \Gamma_1^2, \text{ piezoelectric} \tag{2d}$$

$$\phi = \frac{1}{R_e}\Gamma_2^2, \text{ electromagnetic} \tag{2e}$$

The net system dissipation coefficient μ is then related to combined mechanical b and electrical ϕ influences. Power generated by the harvester is related to the response velocity $\dot{z}$ via

$$P = |v^2|/R_p = \phi|\dot{z}^2|, \text{ piezoelectric} \tag{3a}$$

$$P = R_e|c^2| = \phi|\dot{z}^2|, \text{ electromagnetic} \tag{3b}$$

The colored stochastic excitation $\zeta(t) = -\ddot{g}$ has correlation function $\langle\zeta(t)\zeta(t^*)\rangle = rD\exp\{-r|t-t^*|\}$, where r is the correlation bandwidth (inverse correlation time) and D is the noise intensity. Power spectral density of the stochastic base excitation is

$$S_{\zeta\zeta}(\omega) = 2D/[1+(\omega/r)^2] \tag{4}$$

and the motion is governed by a 1st order Langevin equation

$$\dot{\zeta} + r\zeta = \rho(t) \tag{5a}$$

$$\langle\rho(t)\rangle = 0, \quad \langle\rho(t)\rho(t^*)\rangle = \delta(t-t^*) \tag{5b}$$

where ρ is a Gaussian white noise process. By similar enlargement of the state space, a stochastic excitation of arbitrary correlation function may be related to a Wiener process [26]. Equation (2) is expressed in Itô stochastic differential form as presented by Eq. (6) [27,28].

$$\mathrm{d}\dot{\mathbf{x}} = \begin{bmatrix} x_2 \\ -V'(x_1) - \mu x_2 + x_3 \\ -rx_3 \end{bmatrix}\mathrm{d}t + \begin{bmatrix} 0 \\ 0 \\ r\sqrt{2D} \end{bmatrix}\mathrm{d}B \tag{6a}$$

$$\mathbf{x} = [x_1, x_2, x_3]^T = [z, \dot{z}, \zeta]^T, \quad \mathrm{d}B/\mathrm{d}t = \rho(t) \tag{6b}$$

In the present work, directly simulated results are obtained by integrating Eq. (6) using the stochastic differential equation (SDE) toolbox in MATLAB with the Euler–Maruyama (E–M) algorithm. The corresponding Fokker–Planck equation governing the pdf $\bar{p}(\mathrm{x}, t)$ is given by [27,28]

$$\frac{\partial\bar{p}}{\partial t} = -x_2\frac{\partial\bar{p}}{\partial x_1} + V'(x_1)\frac{\partial\bar{p}}{\partial x_2} + \mu\frac{(x_2\bar{p})}{\partial x_2} - x_3\frac{\partial\bar{p}}{\partial x_2} + r\frac{\partial(x_3\bar{p})}{\partial x_3} + r^2D\frac{\partial^2\bar{p}}{\partial x_3^2} \tag{7}$$

satisfying $\bar{p}(\mathrm{x}, t) \to 0$ as $|\mathrm{x}| \to \infty$. Stationary solutions to Eq. (7) are analytically possible only for quadratic potentials $V(x_1)$, i.e., linear systems. Other potential forms require evaluation of the bandwidth r in order to engage further investigation of the stationary pdf because various approximation methods suited to particular assumptions and accuracy requirements are available. Since r represents a parameter normalized to the mechanical system's characteristic frequency (i.e., $r = 1$ indicates the noise level begins a 20 dB/decade roll-off at the system's linear natural frequency), one must select the appropriate method to determine an approximate stationary pdf based upon the narrowness or breadth of r with respect to prominent mechanical responses. Our practical interest of this work encourages focus on bandwidths around 1 or less, $r \lesssim 1$, since maximum ambient vibration energy of our target excitation sources is sub-Hz and we envision designing harvesters around the point of elastic instability at which linear natural frequency asymptotically approaches zero (although various design factors may not allow for the limiting case to be practically realized).

A preferred scheme to determine pdf response is therefore a decoupling approximation approach set forth by Hänggi [29], later extended and utilized by collaborators [30,31], and recently employed by Daqaq [16] in studying the bistable inductive generator. For brevity, we present here only the outcome of the method since the technique has been formalized in full by Moss and McClintock [27] and Hänggi and Jung [28]. Past studies have used this pdf approximation technique to investigate chiral symmetry breaking in chemical reactions, laser instability, and crystal formation [23,28,32], but we apply the decoupling method for new insight into nonlinear energy harvester design synthesis near the elastic stability limit. The outcome is an approximate, decoupled stationary pdf $p(x_1, x_2)$ expressed as

$$p(x_1, x_2) = Z^{-1}\exp\{-V(x_1)/\sigma_1\}\exp\{-x_2^2/2\sigma_2\} \tag{8a}$$

$$Z = \int_{-\infty}^{\infty}\int_{-\infty}^{\infty}\exp\{-V(x_1)/\sigma_1\}\exp\{-x_2^2/2\sigma_2\}\mathrm{d}x_1\mathrm{d}x_2 \tag{8b}$$

$$\sigma_1 = (D/\mu)/\{1 + \langle V''(x_1)\rangle/[\mu r + r^2]\} \tag{8c}$$

$$\sigma_2 = (D/\mu)/\{1 + \mu/r + \langle V''(x_1)\rangle/r^2\} \tag{8d}$$

$$\langle x_1^2\rangle = \int_{-\infty}^{\infty}\int_{-\infty}^{\infty} x_1^2 p(x_1, x_2)\mathrm{d}x_1\mathrm{d}x_2 \tag{8e}$$

$$\langle x_2^2\rangle = \int_{-\infty}^{\infty}\int_{-\infty}^{\infty} x_2^2 p(x_1, x_2)\mathrm{d}x_1\mathrm{d}x_2 \tag{8f}$$

Here, Z is a normalization constant. In applying the above approximation scheme for the bistable inductive generator, Daqaq [16] noted the challenges involved in determining the decoupled pdf $p(x_1, x_2)$ since it necessitates computation of σ_1 which is a function of the mean-square displacement $\langle x_1^2\rangle$, via $\langle V''(x_1)\rangle$, which is itself dependent on the pdf. Consequently, Daqaq [16] demonstrated the use of an iterative computational method to resolve the circular-dependence concern, and this method was shown to be accurate with respect to direct integration of the SDE. Likewise, we employ the computational method—here, MATLAB command fsolve—to determine solutions to equation system, Eq. (8). Our interest is the generated power of the harvester, Eqs. (3*a*) and (3*b*), which is proportional to the square of the device velocity for both transductions. Therefore, to evaluate the advantages of designing the harvester nonlinear restoring potential around the region of elastic instability when the system is excited by colored noise, we seek insight into the mean-square velocity $\langle x_2^2\rangle$, Eq. (8*f*), following that $\langle P\rangle \propto \langle x_2^2\rangle$.

3 Preliminary Remarks on Accuracy, Comparisons, and Experimentation

The accuracy of the decoupling approximation in predicting mean-square responses is excellent so long as bandwidth r is not too small and noise intensity D is not too large [28,31]. However, accuracy is maintained even for small r so long as noise level is limited $D \lesssim 0.3$ [31]. Results for high bandwidth $r \gg 1$ (white noise limit) correctly converge to Gaussian response estimates, and predictions for quadratic potentials (linear systems) also lead to accurate mean-square responses. Direct simulation of Eq. (6) is complicated by the extremely small time steps required to maintain E–M algorithm stability and the need to integrate for long times in order to obtain reliable mean-square values. In this work, results from 80 simulations each lasting 4000 natural periods are averaged to yield one numerical validation data point; it was observed that significant deviation in results were obtained if less exhaustive number of simulations were averaged. Likewise, experimental results necessitate long evaluation times to attain consistent mean-square responses. These challenges indicate that the greatest number of comparisons among results will help to ensure that the insights obtained are valid to the highest degrees of confidence, and justifies our collective usage of analytical, numerical, and experimental findings.

The experimental setup is shown in Fig. 2 and a schematic is given in the inset of Fig. 3. The cantilevered ferromagnetic spring steel beam has length $L = 132$ mm, width 12.7 mm, and thickness 0.51 mm, and is oriented such that gravity plays no role in the axis of motion. Piezoelectric PVDF patches of length 38 mm and width

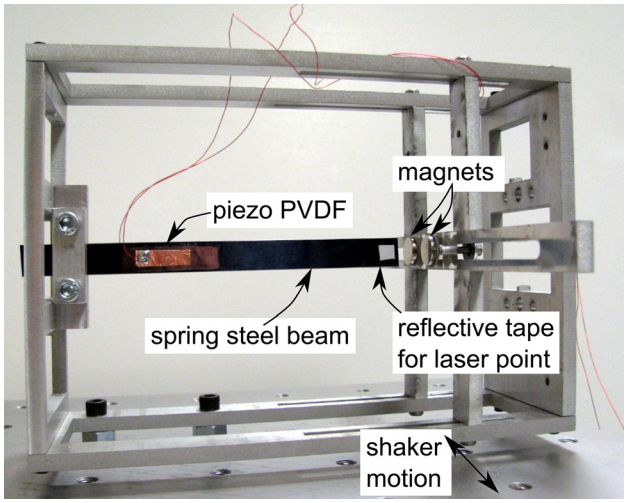

Fig. 2 Cantilevered ferromagnetic beam with PVDF patch and adjustable attractive magnets, attached to electrodynamic shaker

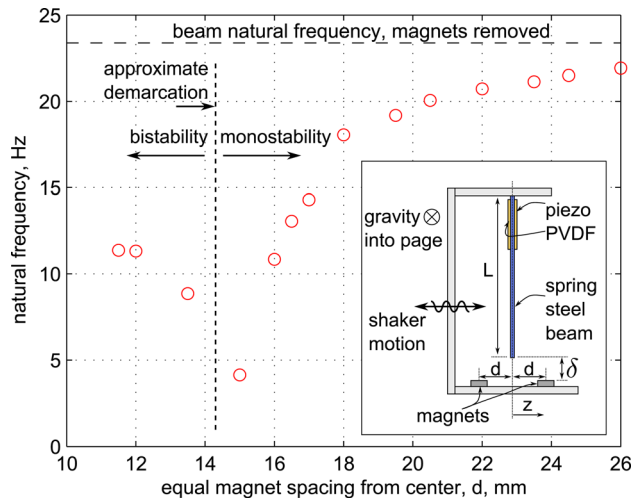

Fig. 3 Measured natural frequencies of beam as equal magnet spacing d is adjusted. Inset shows test schematic

11 mm are applied to both sides of the beam near the clamped end—with poling directions extending away from the beam surfaces—and with electrode leads connected in series to a load resistance of 5.4 M Ω. The magnets are neodymium with diameter 12.7 mm, thickness 6.35 mm, and flux density 1.42 T (as quoted by distributor), and are positioned $\delta = 8$ mm away from the beam free end throughout experimentation; only magnet spacing distance d is adjusted to tailor the harvester restoring potential. In the course of changing magnet position in the range of elastic instability, large changes in natural frequency are observed, Fig. 3. As compared to the beam natural frequency of 23.38 Hz when the magnets are removed (here defined as the linear case), the closest to essential nonlinearity the authors could achieve with the experimental system was a nonlinear monostable beam having natural frequency 4.141 Hz ($d = 15$ mm, Fig. 3), which the authors hereafter refer to as the *essentially nonlinear* case. A ring-down response of the essentially nonlinear harvester is shown in Fig. 4 to exemplify the extremely low frequency oscillations. In the following section, we compare the essentially nonlinear harvester design to a very weakly bistable device. In the bistable configuration, the magnets are positioned equally apart from the beam center position, $d = 13.5$ mm (8.853 Hz intrawell natural frequency), which was the "weakest" and most symmetric bistable configuration the authors could obtain. The stable equilibria of this harvester configuration displaced the beam free end by just +/− 3 mm as compared to the full 132 mm length. Hereafter, this experimental case is referred to as the *bistable harvester*. We note that the gap between magnet spacing $d = 15$ and $d = 13.5$ mm for the essentially nonlinear and bistable configurations, respectively, was extremely difficult to characterize with confidence in the resulting symmetry. However, no distinctly monostable configurations were obtained with magnet spacing less than $d = 15$ mm, indicating the actual elastic stability limit is crossed for spacing d just less than this value.

When generating colored noise for testing, the bandwidth r refers to a value normalized with respect to the mechanical system; thus, $r = 1$ for the linear harvester has noise bandwidth extending to 23.38 Hz while for the essentially nonlinear case the comparable $r = 1$ band extends to just 4.141 Hz. Employing similarly nondimensionalized bandwidths ensures the most challenging performance comparisons among the various harvester designs are made, although final remarks on this stringent comparison method are given later in this work. After selecting the appropriate bandwidth, colored noise is generated by solving Eq. (5) using Runge–Kutta numerical integration. The result is recorded in an uncompressed audio file (300 second length) and played back as input to the electrodynamic shaker amplifier using various excitation levels. Noise intensity level D is determined following experimentation by fitting a power spectral density curve from Eq. (4) to the measured input acceleration spectrum; the results for noise intensity D are then used in analysis and simulation for improved comparison.

4 Noise Bandwidth and Level Influences on Ideal Designs

Figure 5 presents a collection of analytical, numerical, and experimental findings of harvester mean-square velocity—proportional to generated power by Eq. (3*a*)—normalized to noise correlation maxima rD as a function of bandwidth r. In Figs. 5(*a*) and 5(*b*), numerical validations are filled-in marks on the plots. Row (*a*) and (*b*) presents the analytical and numerical results while row (*c*) and (*d*) shows experimental findings with legends indicating the mean-square acceleration input noise levels to provide a more intuitive interpretation of the excitation levels employed. Column

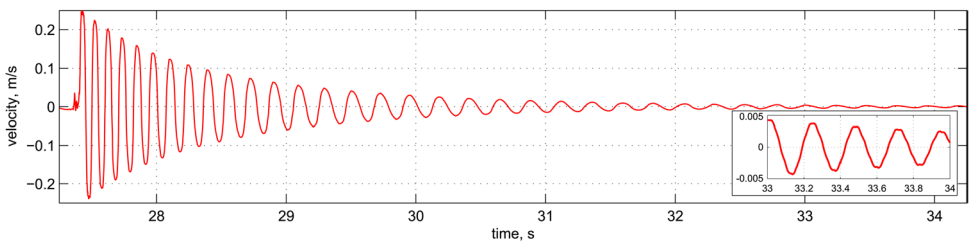

Fig. 4 Beam velocity ring-down response for case of magnet spacing $d = 15$ mm, near point of essential nonlinearity

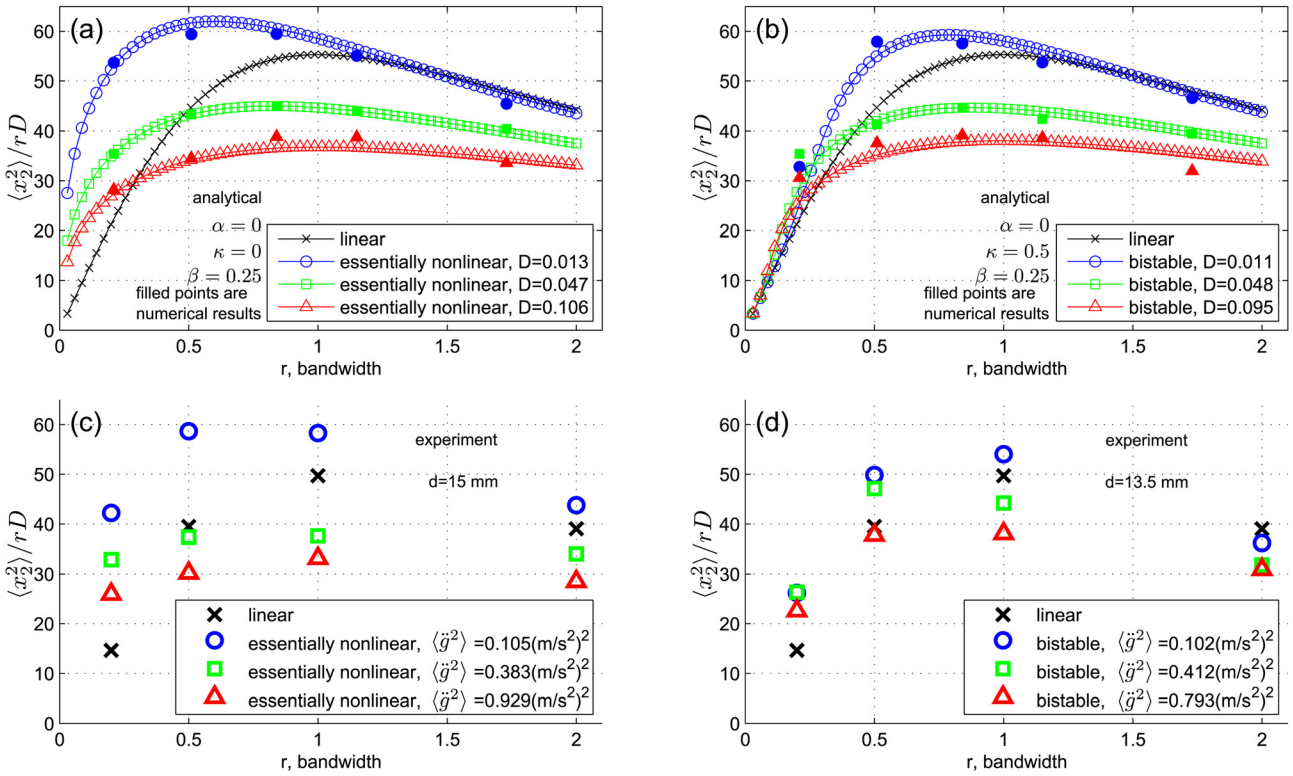

Fig. 5 Harvester mean-square velocity normalized to noise correlation maxima. Row (*a*) and (*b*) analytical results and simulated data (filled-in marks). Row (*c*) and (*d*) experimental results with legends indicating mean-square noise input acceleration values.

(*a*) and (*c*) gives results for the essentially nonlinear harvester and column (*b*) and (*d*) presents bistable harvester data. Results for the linear systems are given on each plot in Fig. 5; in analysis the linear results ($\kappa = -1$, $\alpha = \beta = 0$) are independent of excitation level whereas the linear experimental data represent values averaged over three measured excitation levels which were found to yield very similar ratios of mean-square velocity to noise characteristics rD. Damping of the system is experimentally determined to be $\mu = 0.009$ (combined mechanical and electrical dissipation) and the value is correspondingly used in all subsequent analysis and simulation. The restoring potential parameters κ and β which are employed represent harvesters designed near the elastic stability limit but, lacking comprehensive justification for their specific quantitative values, we are only interested here in qualitative comparison of the experimental data to analytical and numerical results.

Figures 5(*a*) and 5(*b*) show that the peak responses of essentially nonlinear and bistable harvesters are very similar for each level of noise. For low noise levels, there are certain bandwidths for which both nonlinear configurations perform better than the linear counterpart, particularly for noise bandwidths less than the individual systems' natural frequencies, $r < 1$. The peak of the linear harvester velocity responses normalized to excitation parameters rD occurs at $r = 1$, representative of the fact that maximum performance of a linear harvester in colored noise environments for given noise level is obtained so long as the natural frequency of the system is included within the noise bandwidth. In contrast, the essentially nonlinear and bistable harvesters need not have excitation bandwidth extend to their linear resonance frequencies and in fact achieve optimized performance for bandwidths less than this frequency; these optima shift as functions of noise level. Importantly, the essentially nonlinear harvester provides substantially improved power generation when excited by almost any noise level environment having low bandwidths, Figs. 5(*a*) and 5(*c*) $r \lesssim 0.5$. In comparison to the essentially nonlinear harvester, the bistable system has a serious degradation of performance at low excitation bandwidths for all excitation levels, Fig. 5(*b*) $r \lesssim 0.3$, indicating the system is more likely to remain confined to a single well such that its response levels mostly converge to those of the linear harvester. In experiments, the bistable device still provides mild increase in response levels over the linear system at very low bandwidths due to occasional well-escape, Fig. 5(*d*). As both excitation level and bandwidth increase, the performance improvements of the essentially nonlinear and bistable harvesters against the linear counterpart are increasingly degraded. This is explained by the cubic restoring forces of the nonlinear configurations which provide greater resistance to beam displacements in high noise level environments while the linear configuration is not comparatively inhibited.

Simulated results in Figs. 5(*a*) and 5(*b*) show excellent quantitative agreement with analysis. Moreover, all of the key trends of analysis are captured by the experiments, Figs. 5(*c*) and 5(*d*), notably including the superior response levels of the essentially nonlinear harvester in low excitation bandwidth environments at *any* excitation level. These findings indicate that in practical applications for which the ambient vibration spectrum begins a roll-off at extremely low frequencies (characteristic of many real-world excitations like wave or structural vibrations), it may be best to employ an essentially nonlinear harvester given practical constraints of designing linear systems having resonances in such a band.

5 Criticality of Design at the Elastic Stability Limit

Although best performance was obtained by the essentially nonlinear system in Fig. 5 in analysis, simulation, and experiment, our experimental sample is not strictly "essentially nonlinear": given its nonzero linear natural frequency, the system is actually very slightly nonlinear monostable. This returns us to a similar conclusion as that reached by Tang et al. [13] where it was experimentally observed that the "monostable-to-bistable" transition region yielded optimal harvesting performance in *white noise*

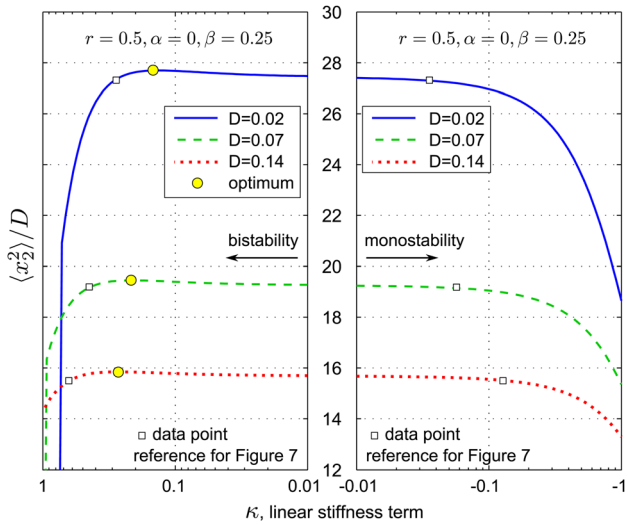

Fig. 6 Influence of linear stiffness term κ on harvester mean-square velocity normalized to excitation level

environments. Yet, if the transition itself appears to be a very high-performance design and there remains difficultly in realizing ideal essential nonlinearity in practice, one must ask whether it makes any difference to defer harvester design towards either mono- or bistability when targeting for the elastic stability limit. Therefore, we now consider how response characteristics are influenced as the linear stiffness term κ is perturbed away from essential nonlinearity, $\kappa = 0$.

Figure 6 plots the influence of the linear stiffness term κ on excitation-normalized harvester velocity response levels. Note that ideal essential nonlinearity corresponds to the region between left and right plots. It is seen that energy harvester performance is substantially unaffected whether the system is designed just before or beyond the critical buckling load. This corroborates similar experimental findings by Tang et al. [13] who employed *white noise* excitations. However, the logarithmic scaling of the horizontal axis may be misleading because adjustment of buckling force—whether attractive magnets, repulsive magnets, or mechanical axial load—is difficult to finely control in close proximity to the elastic stability limit, particularly just beyond the critical buckling load. As shown in Fig. 3 and also discussed by Masana and Daqaq [10], the system may rapidly switch from mono- to bistability. Then, considering Fig. 6 near values $\kappa = \pm 1$, we see that bistable harvester performance plummets for low noise levels. This is the consequence of confinement to a single well and subsequent imposition of *additional intrawell stiffnesses* which raise the linearized natural frequency to $\approx \sqrt{2\kappa}$ [16]; this is a vulnerability that does not concern the slightly monostable harvester since the linear natural frequency remains $\sqrt{|\kappa|}$. While bistable harvester response levels are mostly flat and indicate slightly optimizable configurations (corresponding to optimum escape rates [16]) prior to dropping off rapidly for higher κ (right to left from center), the monostable responses slowly but steadily reduce for any increase in $-\kappa$ (left to right from center). However, because the nonlinear monostable harvester does not exhibit the precipitous drop in response levels and given the difficulty in finely tuning buckling loads at the critical point, monostable systems designed near the elastic stability limit have a distinct robustness advantage.

6 Impact of Asymmetry on Energy Harvesting Performance

In fabricating energy harvesters with restoring potentials configured near the elastic stability limit, numerous practical implementation issues may lead to asymmetric potentials. Therefore, for the experimental results in Fig. 5, both samples may not be precisely symmetric. Following assessment of the comparable importance of obtaining exact essential nonlinearity in Sec. 5, we now address a similar question: to what degree should asymmetry concern energy harvesting design in the region of elastic instability?

Figure 7(*a*) presents analytical results of the excitation-normalized harvester velocity response levels in consequence to changing asymmetric bias α. Several excitation levels D are shown. Given that our experimental sample classified as "essentially nonlinear" was actually slightly monostable, we begin from comparisons of baseline symmetric harvesters with very minor mono- and bistability and perturb these via an asymmetric bias. Due to findings in Fig. 6 where linear stiffness κ was shown to influence the ideal symmetric responses, the system responses in Fig. 7(*a*) are computed with different linear stiffness κ such that their normalized response levels are identical for the case of no bias terms $\alpha = 0$; the baseline starting values are comparatively depicted in Fig. 6 and numerically given in Fig. 7(*a*). In this way,

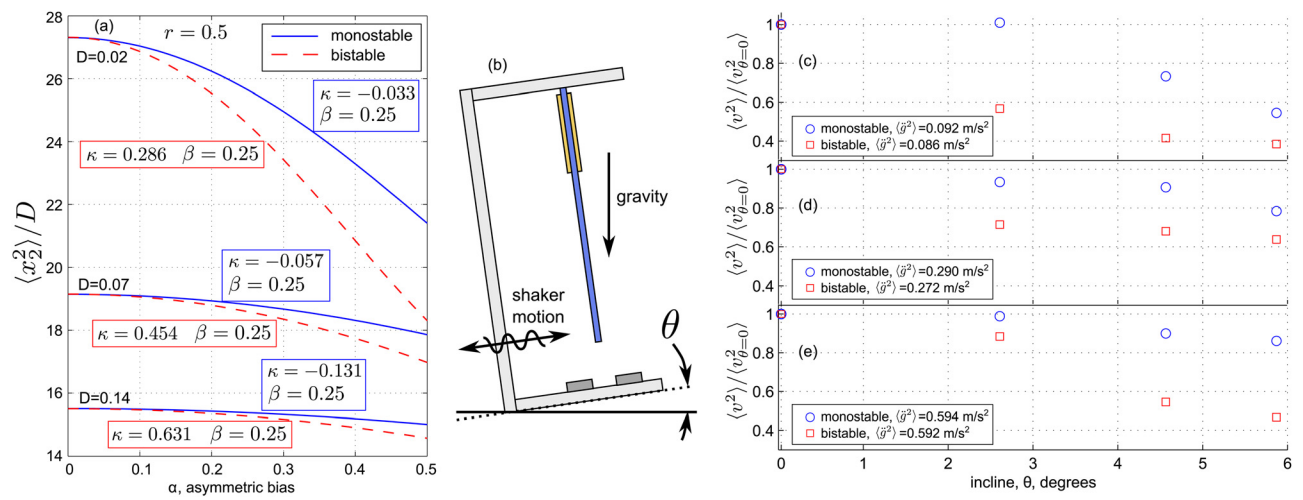

Fig. 7 Influence of bias α on harvester mean-square velocity normalized to excitation level. (*a*) Analysis; (*b*) experimental setup for evaluating influence of gravitational bias; and (*c*)–(*e*) experimental harvester mean-square voltage responses normalized to data for inclination $\theta = 0$ using increasing noise excitation levels from (*c*) to (*e*). Legends indicate mean-square base acceleration levels for each test.

a more meaningful sensitivity comparison is provided since baseline response levels are the same.

Figure 7(*a*) reveals that an asymmetric bias is uniformly more detrimental to a bistable energy harvester's power generation capacity than it is for a slightly monostable system. In perturbing both systems from ideal configurations, the vulnerability of the bistable system to become confined to an individual intrawell response, and the subsequent additional stiffnesses associated with this deviation, suggest that bistable energy harvesting systems have a distinct disadvantage. The influence of asymmetry is far more pronounced at low excitation levels, indicating well-escape is greatly inhibited for the bistable configuration in such cases. Yet, regardless of excitation level, the asymmetric nonlinear monostable system is less susceptible to performance degradation due to the same degree of bias.

To validate these predictions, we consider the influence of gravitational bias on the test setup. To accomplish this, the test fixture is arranged with the harvester beam free end hanging downward but inclined from the vertical direction (gravitational force direction), Fig. 7(*b*). The shaker force direction is along the beam's axis of transverse motion, inclined from the horizontal plane with angle θ. By changing the inclination, θ, the linear and cubic restoring force terms proportional to κ and β are held constant since magnet spacing remains fixed. The responses of a nonlinear monostable harvester with equal magnet spacing $d=16$ mm are compared to a bistable configuration with magnet spacing $d=13.5$ mm. Both experimental samples represent nonlinear harvesters having restoring potentials slightly perturbed from essential nonlinearity (Fig. 3). The piezoelectric PVDF voltage output serves as the response signal and these values are normalized with respect to measurements taken without inclination, $\theta=0$ deg; thus, data points for both systems coincide at $\theta=0$.

Figures 7(*c*)–7(*e*) show experimental results for steadily increasing colored noise ($r=0.5$) base acceleration levels. Mean-square excitation levels for each test are provided in the corresponding legends and each test captured 500 seconds of data. The first inclination of 2.6 deg leads to notable and uniform reductions in bistable harvester responses, regardless of noise excitation level. In contrast, the smallest inclination has comparatively little effect, if any, on the monostable device. Only for inclines of 4.5 and 5.9 deg do the monostable harvester responses begin to degrade. At low noise levels, Fig. 7(*c*), the reduced response levels are most pronounced for both systems. In comparison to the bistable system levels, however, the monostable harvester exhibits substantially less performance reduction. These findings are in good qualitative agreement with predictions in Fig. 7(*a*). It was confirmed that for an inclination of 5.9 deg the bistable device still exhibited static bistability; yet, only occasional cross-well escape events were observed during tests at 5.9 deg even for higher excitation levels. Intuitively, the results demonstrate that the addition of a *potential barrier* for the bistable harvester is a nontrivial detriment to power generation in stochastic environments when asymmetries become manifest.

7 Conclusion

Adopting a practical design approach to vibrational energy harvesting from realistic ambient vibration sources, this work has sought to shed valuable light on some of the more promising opportunities provided by shaping the restoring potential of nonlinear harvesters in the region of elastic instability. An established stationary pdf approximation technique is utilized to predict harvester dynamics in response to colored noise excitations, and series of simulated and measured data are compared against the analyses. The analytical, numerical, and experimental results exhibit very good agreement, which help to comprehensively support the overall conclusions of this research. Several critical insights may be drawn from these investigations.

One may reason from Fig. 5 that a linear harvester, having independence of normalized response level to changing noise level, is a better choice as compared to devices designed near the elastic stability limit. However, as vividly depicted in Fig. 3 in comparing the natural frequencies of the measured systems and as recognized by Daqaq [16], a linear "version" of a given harvester may have natural frequency far removed from the nonlinear counterpart. Thus, results in Fig. 5 contrasting several nonlinear designs to the linear case must be carefully assessed when comparing systems excited by the same noise level. Consider a bridge having lowest natural frequency near 0.8 Hz [2]. For our "essentially nonlinear" test system with natural frequency 4.141 Hz, this represents a bandwidth $r\approx 0.19$, while for the linear counterpart having natural frequency 23.38 Hz, this is a bandwidth of $r\approx 0.03$. Thus, a direct comparison between the two designs necessitates determining the mean-square response of the essentially nonlinear harvester for $r\approx 0.19$, $\langle x_2^2\rangle/rD\approx 52.3$ (Fig. 5(*a*) for $D=0.013$), and comparing to the linear system response for $r\approx 0.03$, $\langle x_2^2\rangle/rD\approx 3.32$. Therefore, the essentially nonlinear harvester would generate about 16 times more power than the linear version. This is an extreme example given the great disparity between the natural frequencies, but it helps to exemplify the fact that taking steps to shape the restoring potential of an energy harvesting system to be most sensitive to the realistic forms and spectra of ambient vibration is key to successful power generation.

Therefore, to best match harvester design to common, ambient colored noise excitations, the lowest achievable natural frequency is necessary, but the importance of utilizing the popular bistable configuration is not critical. While a very weakly bistable device is shown to yield comparable (or even slightly better) response levels than a slightly nonlinear monostable system designed near the elastic stability limit (Fig. 6), practical concerns regarding asymmetry and the need for a priori knowledge of excitation level, which may both lead to single-well confinement and corresponding stiffening effects, suggest there are more issues in employment of bistable harvesters than nonlinear monostable devices.

This work demonstrated that ideal, essentially nonlinear energy harvesters appear as a potent solution to power generation from realistic ambient vibrations. By eliminating linear restoring forces, the essentially nonlinear design comes as close to a pure electrical damper as possible in low excitation level environments (which induce small displacements about equilibrium). However, in the absence of ideal design at the precise limit of elastic stability, erring on the side of nonlinear monostability appears to be a wiser decision than obtaining bistability due to the latter's performance vulnerability in consequence to single-well confinement which introduces additional stiffening into the system. The optimal *performance* may be attained with weakly bistable systems, but in practical applications a critical need for system *robustness* dictates avoiding crossing the elastic stability limit and retaining monostability if ideal essential nonlinearity is not realizable.

References

[1] Cruz, J., 2008, *Ocean Wave Energy: Current Status and Future Perspectives*, Springer, Berlin.

[2] Shama, A. A., Mander, J. B., Chen, S. S., and Aref, A. J., 2001, "Ambient Vibration and Seismic Evaluation of a Cantilever Truss Bridge," Eng. Struct., **23**, pp. 1281–1292.

[3] Albers, W. F., Hag-Elsafi, O., and Alampalli, S., 2007, "Dynamic Analysis of the Bentley Creek Bridge With FRP Deck," U.S. Department of Transportation Federal Highway Administration, Report No. SR-07/150.

[4] Kumarasena, S., Jones, N. P., Irwin, P., and Taylor, P., 2007, "Wind-Induced Vibration of Stay Cables," U.S. Department of Transportation Federal Highway Administration, Report No. FHWA-RD-05-083.

[5] Dykman, M., and Lindenberg, K., 1994, "Fluctuations in Nonlinear Systems Driven by Colored Noise," *Contemporary Problems in Statistical Physics*, Weiss G.H., ed., SIAM, Philadelphia.

[6] Zhu, D., Tudor, M. J., and Beeby, S. P., 2010, "Strategies for Increasing the Operating Frequency Range of Vibration Energy Harvesters: A Review," Meas. Sci. Technol., **21**, p. 022001.

[7] Harne R. L., and Wang, K. W., 2013, "A Review of the Recent Research on Vibration Energy Harvesting Via Bistable Systems," Smart Mater. Struct., **22**, p. 023001.

[8] Stanton, S. C., McGehee, C. C., and Mann, B. P., 2010, "Nonlinear Dynamics for Broadband Energy Harvesting: Investigation of a Bistable Piezoelectric Inertial Generator," Phys. D., **239**, pp. 640–653.
[9] Erturk, A., and Inman, D. J., 2011, "Broadband Piezoelectric Power Generation on High-Energy Orbits of the Bistable Duffing Oscillator With Electromechanical Coupling," J. Sound Vib., **330**, pp. 2339–2353.
[10] Masana, R., and Daqaq, M. F., 2012, "Energy Harvesting in the Super-Harmonic Frequency Region of a Twin-Well Oscillator," J. Appl. Phys., **111**, p. 044501.
[11] Quinn, D. D., Triplett, A. L., Bergman, L. A., and Vakakis, A. F., 2011, "Comparing Linear and Essentially Nonlinear Vibration-Based Energy Harvesting," ASME J. Vib. Acoust., **133**, p. 011001.
[12] Quinn, D. D., Triplett, A. L., Vakakis, A. F., and Bergman, L. A., 2011, "Energy Harvesting from Impulsive Loads Using Intentional Essential Nonlinearities," ASME J. Vib. Acoust., **133**, p. 011004.
[13] Tang, L., Yang, Y., and Soh, C-K., 2012, "Improving Functionality of Vibration Energy Harvesters Using Magnets," J. Intell. Mater. Syst. Struct., **23**(13), pp. 1433–1449.
[14] Zhao, S., and Erturk, A., 2013, "On the Stochastic Excitation of Monostable and Bistable Electroelastic Power Generators: Relative Advantages and Tradeoffs in a Physical System," Appl. Phys. Lett., **102**, p. 103902.
[15] Daqaq, M. F., 2010, "Response of Uni-Modal Duffing-Type Harvesters to Random Forced Excitations," J. Sound Vib., **329**, pp. 3621–3631.
[16] Daqaq, M. F., 2011, "Transduction of a Bistable Inductive Generator Driven by White and Exponentially Correlated Gaussian Noise," J. Sound Vib., **330**, pp. 2554–2564.
[17] Daqaq, M. F., 2012, "On Intentional Introduction of Stiffness Nonlinearities for Energy Harvesting Under White Gaussian Excitations," Nonlinear Dyn., **69**, pp. 1063–1079.
[18] Meimukhin, D., Cohen, N., and Bucher, I., 2013, "On the Advantage of a Bistable Energy Harvesting Oscillator Under Bandlimited Stochastic Excitation," J. Intell. Mater. Syst. Struct., **24**, pp. 1736–1746.
[19] Green, P. L., Papatheou, E., and Sims, N. D., 2013, "Energy Harvesting From Human Motion and Bridge Vibrations: An Evaluation of Current Nonlinear Energy Harvesting Solutions," J. Intell. Mater. Syst. Struct., **24**, pp. 1494–1505.
[20] Cohen, N., Bucher, I., and Feldman, M., 2012, "Slow-Fast Response Decomposition of a Bi-Stable Energy Harvester," Mech. Syst. Signal Process., **31**, pp. 29–39.
[21] Sneller, A. J., Cette, P., and Mann, B. P., 2011, "Experimental Investigation of a Post-Buckled Piezoelectric Beam With an Attached Central Mass Used to Harvest Energy," Proc. Inst. Mech. Eng., Part I: J. Syst. Control Eng., **225**, pp. 497–509.
[22] Harne, R. L., Thota, M., and Wang, K. W., 2013, "Concise and High-Fidelity Predictive Criteria for Maximizing Performance and Robustness of Bistable Energy Harvesters," Appl. Phys. Lett., **102**, p. 053903.
[23] Kondepudi, D. K., Prigogine, I., and Nelson, G., 1985, "Sensitivity of Branch Selection in Nonequilibrium Systems," Phys. Lett. A, **111**, pp. 29–32.
[24] Kondepudi, D. K., Moss, F., and McClintock, P. V. E., 1986, "Branch Selection in the Presence of Coloured Noise," Phys. Lett A, **114**, pp. 68–74.
[25] Liao, Y., and Sodano, H. A., 2009, "Structural Effects and Energy Conversion Efficiency of Power Harvesting," J. Intell. Mater. Syst. Struct., **20**, pp. 505–514.
[26] Risken, H., 1989, *The Fokker-Planck Equation: Methods of Solution and Applications*, 2nd ed, Springer-Verlag, Berlin.
[27] Moss, F., and McClintock, P. V. E., eds., 1989, *Noise in Nonlinear Dynamical Systems, Volume 1: Theory of Continuous Fokker-Planck Systems*, Cambridge University, Cambridge, UK.
[28] Hänggi, P., and Jung, P., 1995, "Colored Noise in Dynamical Systems,", I. Prigogine and S. A. Rice, eds., *Advances in Chemical Physics*, Vol. 89, Wiley, New York, pp. 239–326.
[29] Hänggi, P., 1978, "Correlation Functions and Master Equations of Generalized (Non-Markovian) Langevin Equations," Z. für Physik B, **31**, pp. 407–416.
[30] Hänggi, P., Mroczkowski, T. J., Moss, F., and McClintock, P. V. E., 1985, "Bistability Driven by Colored Noise: Theory and Experiment," Phys. Rev. A, **32**, pp. 695–698.
[31] Fronzoni, L., Grigolini, P., Hänggi, P., Mannella, R., and McClintock, P. V. E., 1986, "Bistable Oscillator Dynamics Driven by Nonwhite Noise," Phys. Rev. A, **33**, pp. 3320–3327.
[32] Moss, F., and McClintock, P. V. E., eds., 1989, *Noise in Nonlinear Dynamical Systems, Volume 3: Experiments and Simulations*, Cambridge University, Cambridge, UK.